I.A.U
Karaj branch

Journal of
A p p l ied
C hemical
R esearch
jacr.kiau.ac.ir

Journal of Applied Chemical Research, 18, 1, 60-71 (2024)

Preparation, Structural and Magnetic Behavior of $Sr(AlCr)_xFe_{(12-2x)}O_{19}$ Hexagonal Ferrites

Mahboobeh Alimoradi[1], Mohammad Yousefi[2*], Babak Sadeghi[3], Mostafa M.Amini[4] Alireza Abbasi[5]

[1]Department of Chemistry, Science and Research Branch, Islamic Azad University, Tehran, Iran

[2]Department of Chemistry, Faculty of Pharmaceutical Chemistry, Tehran Medical Sciences,Islamic Azad University, Tehran, Iran

[3]Department of Chemistry, Tonekabon Branch, Islamic Azad University, Tonekabon, Iran

[4]Department of Chemistry, Shahid Beheshti University, G.C., Tehran, Iran

[5]School of Chemistry, College of Science,University of Tehran, Tehran, Iran

(Received 24 May 2023; Final revised received 17 Aug. 2023)

Abstract

In this investigation, strontium hexaferrite nanocomposites co-doped with aluminum and chromium were prepared $Sr(AlCr)_xFe_{(12-2x)}O_{19}$ with x different amounts (x= 0, 0.2, 0.4, 0.6 and 0.8), were synthesized. The magnetic nanocomposites have been prepared by simple sol-gel auto-combustion method. The morphology and structure of nano-samples were determined by FTIR, XRD and FE-SEM . The results of the XRD pattern confirmed P63/mmc space group and the single phase of the synthesized samples. The crystal size of the prepared samples decreases with increasing Al and Cr. The magnetic properties of these compounds are determined by the VSM. Magnetic properties (M_r, M_s and Hc) were measured. The result showed that M_r and M_s decrease with the increase of Al and Cr.

Keywords: Nano composite, M-type hexaferrite, Sol-gel processes, Magnetic properties.

***Corresponding author:** Mohammad Yousefi, Department of Chemistry, Faculty of Pharmaceutical Chemistry, Tehran Medical Sciences, Islamic Azad University, Tehran, Iran, E-mail: myousefi50@hotmail.com.*

Introduction

As we can see the evolution of electronic systems, wireless devices, modern radio equipment, electronics, cell phones, Wi-Fi equipment have made life much easier, but they have also created dangers to human health [1]. They cause contaminants such as electromagnetic interference (EMI). In this situation, it is necessary to find new materials for the absorption of electromagnetic waves with high potency and appropriate index. One of the most efficient methods is the absorption of electromagnetic waves by some materials. In recent decades, numerous studies have been conducted on magnetic hexaferrite materials, applied in telecommunications and microwave radar systems because of their great tunable anisotropy field [2].

M-type hexaferrites (M = Sr, Ba, Pb, and Ca) are known to belong to an important classification of magnetic materials variably applied in recording media, permanent magnets, microwave device [3, 4], drug delivery [5], biomedical applications [6]. M-type hexaferrite is a hard magnetic material, specified by low-saturation magnetization property [7], excellent chemical stability [8], and low cost [9]. These materials have a magneto plumbite structure displayed as a sequence of hexagonal and spinel blocks, alternating along the c axis and containing a large number of Fe^{3+} ions on the crystallographic lattice sites [10]. The pure M- type hexaferrites such as: $BaFe_{12}O_{19}$and $SrFe_{12}O_{19}$, have high a magnetic resonance frequency about 47 GHz. In order to control the shift in the frequency of the microwave absorption for the applications in the frequency range of 8–18 GHz; doping other elements into M- type hexaferrite has been considered [11, 12]. Added doping reduces the frequency of high magnetic resonance and increases the electrical properties and are modified the magnetic properties of hexaferrite [13].

Hence, the aim of the current study was established based on the effect of various dopants (Al and Cr) concentrations on the magnetic, morphological, and structural properties of the magnetic nanocomposite. Therefore, five dopant concentrations (x = 0, 0.2, 0.4, 0.6, and 0.8) were applied to synthesized $Sr(AlCr)_xFe_{(12-2x)}O_{19}$ nanocomposites through the sol-gel auto-combustion method. The structure of synthesized magnetic compounds properties was determined by IR, XRD, FESEM and VSM.

Experimental

Materials

Iron nitrate ($Fe(NO_3)_3.9H_2O$), strontium nitrate ($Sr(NO_3)_2.6H_2O$), aluminum nitrate ($Al(NO_3)_3.9H_2O$), chrome nitrate ($Cr(NO_3)_3.6H_2O$), and citric acid ($C_6H_8O_7.H_2O$) used in this research were purchased from Merck company. In this research, all of the reagents were analytically graded and all chemicals were used without any further purification.

Preparation of hexagonal ferrite $Sr(AlCr)_xFe_{(12-2x)}O_{19}$

A series of M-hexagonal ferrites of composition $Sr(AlCr)_xFe_{(12-2x)}O_{19}$(x = 0, 0.2, 0.4, 0.6, and 0.8) were investigated using the sol-gel auto-combustion method. Stoichiometric amounts of raw materials were dissolved in deionized water and then added to the citric acid solution (molar ratio of citric acid to salts was 1.1/1). After about 2 h, ammonium solution was added dropwise to adjust pH at 7-7.5. The solution was heated up to 180 °C. After about a few hours, the solution became viscous and gel formed. Then, combustion occurred automatically and fine powder was gained. then, firstly, the synthesized powder was annealed at 500 °C for 1 h and then calcinated at 900 °C for 2 h to obtain M-hexagonal ferrite. The schematic diagram of the synthesis process is presented in Figure 1.

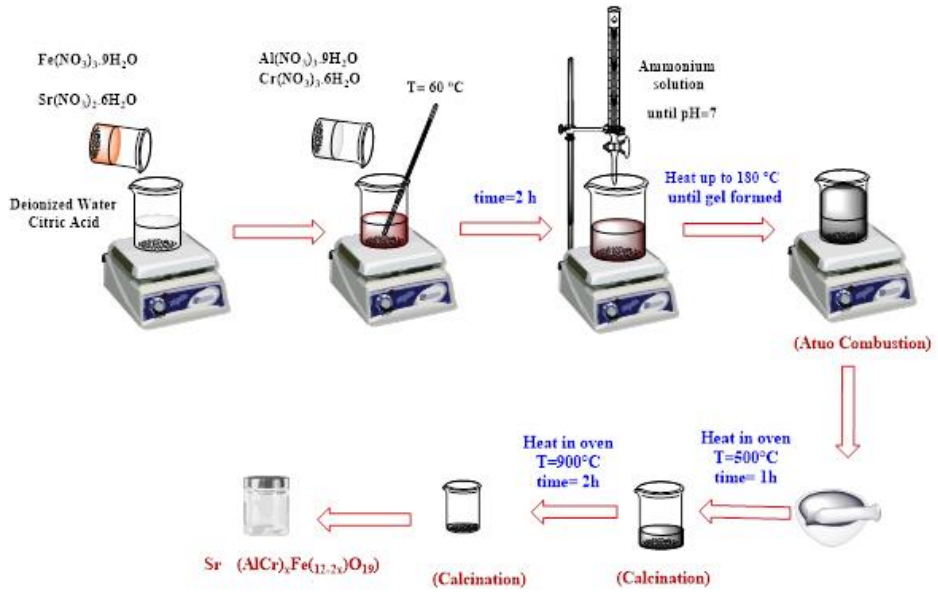

Figure 1. Schematic diagram of samples synthesis of $Sr(AlCr)_xFe_{(12-2x)}O_{19}$(x = 0, 0.2, 0.4, 0.6, and 0.8).

Characterization

The composites formation was confirmed by Fourier transform infrared spectroscopy (FTIR) (Thermo-Nicolet 8700 – FTIR spectrometer) in the range of 400–2000 cm^{-1}. The crystal structure of hexaferrites were carried out by X-ray diffractometer (XRD) (STOE STADIP) with CuKα radiation λ = 0.154 nm and 2θ range from 20 to 80°. Morphologies of the samples were observed by a field emission scanning electron microscope (FESEM) (Zeiss-sigma VP-500). For energy-dispersive X-ray spectroscopy (EDX), analysis was performed with an acceleration voltage of 20

kV. In addition, the magnetic properties were measured by vibrating sample magnetometer (VSM) (Kavir magnet) with magnetic fields from − 15 kOe to + 15 kOe at the temperature room.

Result and discussion

FTIR Analysis

The FT-IR spectra of the synthesized compounds were studied to detect the functional groups and bands in the samples. Table 1 and Figure 2 displays the FT-IR spectrum of synthesized hexaferrite compounds in the range of 400–2000 cm^{-1}.

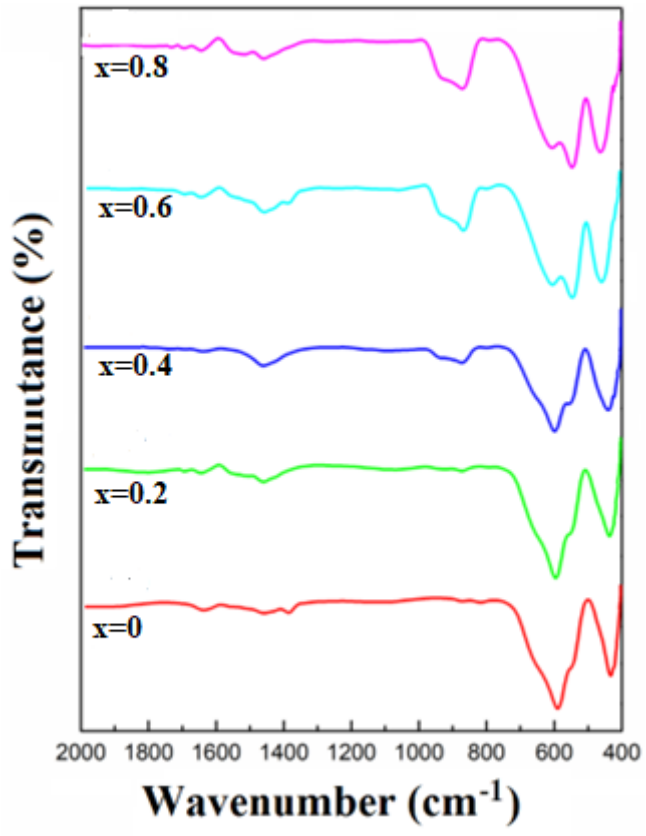

Figure 2. FTIR spectra of $Sr(AlCr)_xFe_{(12-2x)}O_{19}$(x = 0, 0.2, 0.4, 0.6, and 0.8)

The absorption bands in the range of 430–470 cm^{-1} and 540-610 cm^{-1} represent the stretching vibration band of Fe–O, in octahedral and tetrahedral sites, respectively [3, 14]. According to the previous studies, the vibration modes obtained from the tetrahedral clusters are longer than the octahedral clusters [15] due to the shorter lengths of the bands in the tetrahedral clusters. On the other hand, ionic radius of Al^{+3} (0.57 Å) and Cr^{+3} (0.62 Å) differs from the ionic radius of Fe^{+3} (0.645 Å), therefore, the substitution in the structure changes the distribution of Fe^{+3} ions within the

structure, which can affect the displacement of vibration bands. In addition, by increasing the of dopants, the frequency of absorption peaks is shifted to a higher wave number, due to the greater atomic weight of the substituted ions of Al^{+3} (26.98) and Cr^{+3} (51.99) compared to the atomic weight of Fe^{+3} (55.845) [2, 16].

Table 1. Absorption bands of Fe-O vibrations in tetrahedral and octahedral sites of $Sr(AlCr)_xFe_{(12-2x)}O_{19}$(x = 0, 0.2, 0.4, 0.6, and 0.8).

$Sr(AlCr)_xFe_{(12-2x)}O_{19}$	Band of tetrahedral (cm-1)	Band of octahedral (cm-1)
X=0	578	423
X=0.2	585	432
X=0.4	595	442
X=0.6	602	459
X=0.8	606	461

Phase identification analysis

The structure and crystal shape of the synthesized ferrite compounds were determined by XRD. The XRD patterns of annealed samples are shown in Figure 3. All samples matched with the JCPDS card number 98-004-3590 had space group of $P6_3/mmc$. In all samples, the Fe_2O_3 phase wasn't observed, presumably related to the increasing calcination temperature, which led to the Fe_2O_3 removed and the pure phase of hexaferrite formed [17].

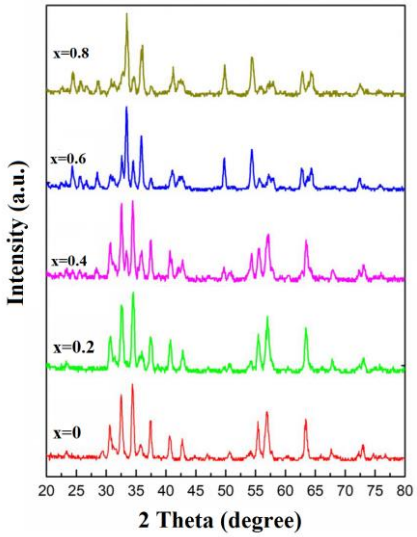

Figure 3. XRD patterns of $Sr(AlCr)_xFe_{(12-2x)}O_{19}$(x = 0, 0.2, 0.4, 0.6, and 0.8).

The main planes of hexaferrite such as (107), (114), (110), and (108) were clearly observed for all of the samples in Figure 3. The relative intensities of the diffraction peaks were maintained with very small changes.

The values of *c/a*, crystallite size and cell volume (*V*) were calculated from the XRD data and tabulated in Table 2. The value of *c/a* is almost constant for all of the samples (lattice parameters (*a*) and (*c*)) and is calculated using the following relation[18]:

$$\frac{1}{d^2} = \frac{4}{3}\left(\frac{h^2 + hk + k^2}{a^2}\right) + \frac{l^2}{c^2}$$

where *d* and (*h k l*) are the crystal phase distance and the Miller index, respectively. The crystallite size particles are also calculated using the Sherrer equation [19]:

$$D\ (h, k, l) = \frac{k\lambda}{\beta \cos\theta}$$

$$V = \frac{\sqrt{3}a^2 c}{2}$$

Where λ = 0.154 nm (the X-ray wavelength), K = 0.89, *ß* is FWHM, and θ is brag angle for *h, k, l* Miller indices.

Table 2. Lattice parameters (*a*, *c*, *c/a*, *V*) and crystallite size of $Sr(AlCr)_xFe_{(12-2x)}O_{19}$ (x = 0, 0.2, 0.4, 0.6, and 0.8)

$Sr(AlCr)_xFe_{(12-2x)}O_{19}$	*a*(Å)	*c*(Å)	*c/a*	*V*(Å^3)	Crystallite size (nm)
X=0	5.87	23.93	3.91	696	39
X=0.2	5.85	23.91	3.92	687	36
X=0.4	5.84	23.84	3.93	681	31
X=0.6	5.70	23.55	3.94	669	28
X=0.8	5.63	23.35	3.96	645	26

As shown in Table 2, it is concluded that the substitution of the cations Al^{+3} and Cr^{+3} causes a very small change in the lattice parameters *a* and *c*. This difference in lattice constant values with the substitution of the desired cations shows that the magnetic axis *c* is more displaced than *an* axis, and this is due to the difference in the ionic radius of the cations Al^{+3} (0.532 Å) and Cr^{+3} (0.52 Å) is relative to Fe^{+3} (0.645 Å). Also, *D* indicates the crystal size of all prepared samples that calculated

by Sherer equation. The *c*/*a* ratio is another important factor involved in determining the structure of M-type hexaferrites. It is usually less than 3.96 for magnetoplambitites, and above this value is for β-alumina [20]. According to Table 2, the *c*/*a* ratio of all synthesized samples correspond to the value for type M hexaferrite. As a result, substitution of Al^{+3} and Cr^{+3} cations in the structure of $SrFe_{12}O_{19}$ did not change the type of this ferrite.

FESEM micrographs

The surface morphology of the $Sr(AlCr)_xFe_{(12-2x)}O_{19}$(x = 0, 0.2, 0.4, 0.6, and 0.8) powder is presented in Figure 4. These images show an almost uniform distribution and hexagonal morphology with well-defined vertices that can be attributed to barium hexaferrite type M particles. More than 90% of the particles have an average size of about 25-40 nm and have a hexagonal morphology. Moreover, the presence of agglomerates is observed in parts of the image that occur from the joining of smaller particles to reduce surface free energy, indicating magnetic interaction between particles, and the decrease in particle size is consistent with the crystal size of the Scherer equation [19, 21].

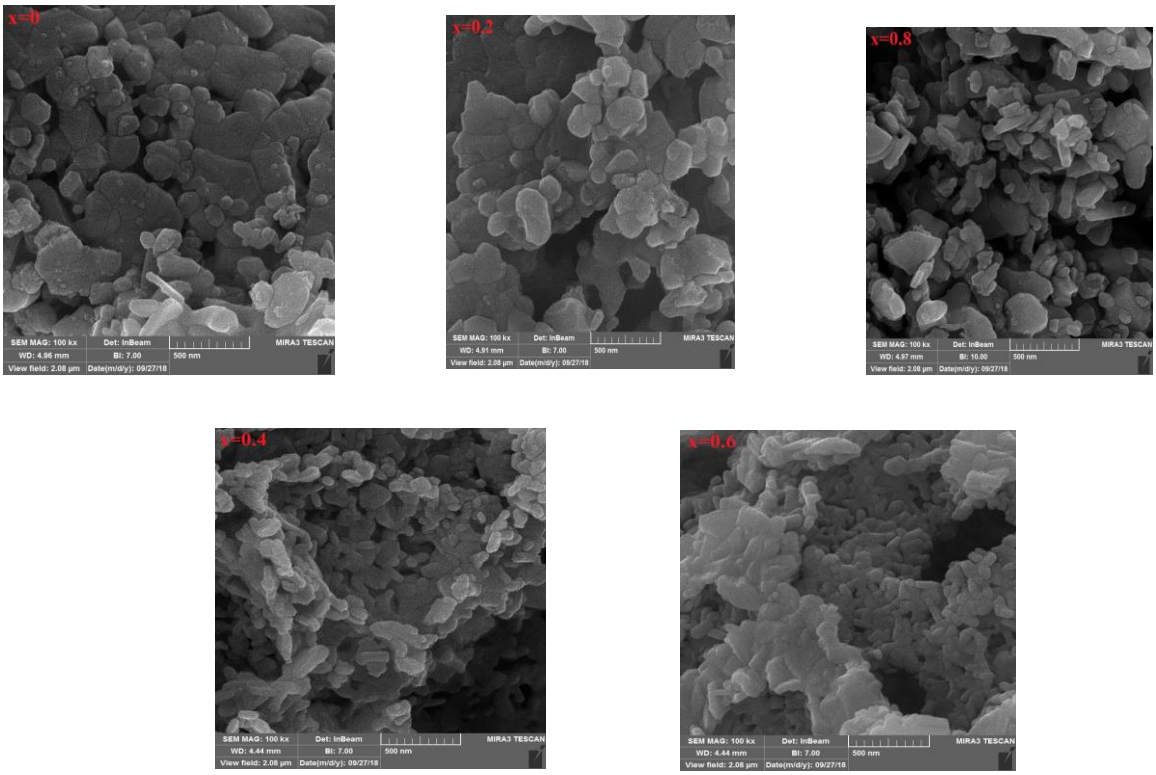

Figure 4. SEM image of $Sr(AlCr)_xFe_{(12-2x)}O_{19}$(x = 0, 0.2, 0.4, 0.6, and 0.8).

Magnetic Properties Analysis

Figure 5 displays the hysteresis loops of the $Sr(AlCr)_xFe_{(12-2x)}O_{19}$(x = 0, 0.2, 0.4, 0.6, and 0.8) Nano hexaferrite at room temperature under the magnetic field in the range of ±15 kOe. The magnetic parameters including saturation magnetization (Ms), coercivity (Hc), remnant magnetization (Mr) and squareness ratio (Mr/Ms), obtained from the hysteresis loops, are depicted in Table 3.

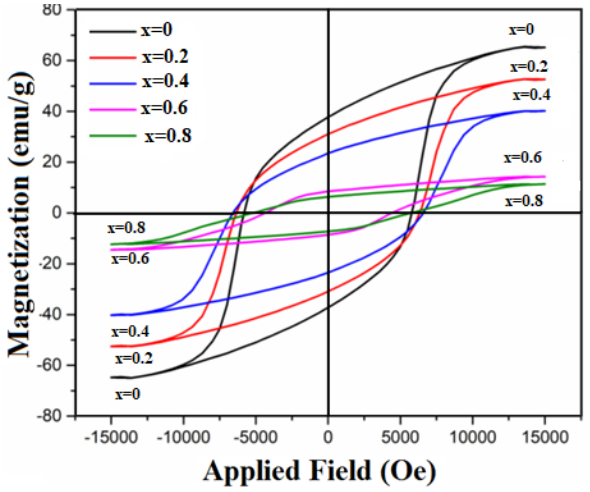

Figure 5. Magnetic hysteresis loops for the composite samples of $Sr(AlCr)_xFe_{(12-2x)}O_{19}$(x = 0, 0.2, 0.4, 0.6, and 0.8).

In all samples, the increasing amount of dopant led to a regular decrease in Ms and Mr values which were consistent with previous studies [22] but the changes of Hc were at first increasing (in **x**=0.2 & 0.4) then decreasing(in **x**=0.6 & 0.8).

The amount of Ms in the pure strontium hexaferrite (**x** = 0) was measured as 63.82 emu/g. This value is then reduced in samples of **x** = 0.2–0.8 by doping of Al^{3+}, Cr^{3+} elements into the structure. In general, the properties of strontium hexaferrite depend on the microstructure, synthesis conditions, electron configuration and occupation of the crystallographic position of Fe^{3+} by various cations, in addition to substitution [23]. The magneto plumbite structure of M-type hexaferrite, is containing RSR*S* blocks (R* and S* are R and S blocks that rotate 180° in the easy axial direction). Twenty-four Fe^{3+} ions are located in five sites in which three of them are octahedral [12k(↑),4f2(↓) and 2a(↓)] sites, one for tetrahedral [4f1(↓)] and one remained sites is for bipyramidal [2b(↑)] [24]. Al^{3+} and Cr^{3+} doped ions considerably decreased the magnetic properties (the decrease of Ms for samples with **x** = 0.2–0.8) due to less magnetic properties than Fe^{3+} ions. The magnetic moment of Cr^{3+} ions was reported 3 μB and Al^{3+} ions have not shown magnetic

properties (0 μB) lower than the magnetic moment of Fe (5 μB) [25]. The saturation magnetization was related to the unpaired electrons. The substitution of cations in the structure of strontium hexaferrite leads to the conversion of Fe^{3+} to Fe^{2+} at sites 2a. As a result, the Ms follows the magnetic dilution phenomenon, because the magnetic properties depend on Fe^{3+}-O-Fe^{2+} super exchange interaction [26].

The value of the squareness ratio (M_r/M_s) in the range of 0.57–0.59 indicates that the material features a single domain magnetic structure and revealed the exchange coupling of particles in all samples [27].

The coercivity (Hc) in the synthesized nanoparticles does not change uniformly. Various parameters such as particle size and crystal defect, etc. affect the value of Hc. But in single-domain magnetic structures, there is an inverse relationship between coercivity and particle size. So first the coercivity will increase and suddenly decrease.

Table 3. Magnetic parameters of $Sr(AlCr)_xFe_{(12-2x)}O_{19}$(x = 0, 0.2, 0.4, 0.6, and 0.8).

$Sr(AlCr)_xFe_{(12-2x)}O_{19}$	***Hc*(Oe)**	***Mr* (emu/g)**	***Ms* (emu/g)**	***Mr*/Ms**
X=0	5873	36.781	63.829	0.57
X=0.2	6324	30.952	53.985	0.57
X=0.4	6562	22.998	39.114	0.59
X=0.6	4567	8.594	14.886	0.58
X=0.8	5698	6.974	12.295	0.57

Conclusion

The main conclusions obtained in this study can be summarized as follows:

1. Five new hexagonal ferrite $Sr(AlCr)_xFe_{(12-2x)}O_{19}$(**x = 0, 0.2, 0.4, 0.6, and 0.8**) were prepared using the sol-gel auto-combustion method.
2. FTIR spectra at 400–600 cm^{-1} corresponded to the tetrahedral and octahedral vibrating modes of Fe-O.
3. The XRD patterns confirmed that the all-crystal structure of the nanocomposite is in good accordance with JPDS file number 98-004-3590 and corresponded to the hexagonal crystal symmetry of the P63/mmc space group. The substitution of two small cationic radii decreased the lattice parameters of a, c compared to the iron.

4. FESEM results showed hexagonal shapes of all samples and particle sizes were calculated 25-40 nm. On the other hand, increasing the concentration of dopants led to irregular shapes and reduced size of the nanoparticles.
5. Magnetization study represented that by substituting dopants in hexaferrite structure, M_s and M_r reduced with increase Al, Cr in hexaferrite structure.
6. Therefore, it is possible to synthesize hexafrites with different elements and polymers and or graphene and compare their magnetic properties. It is also possible to check the property of absorbing electromagnetic waves of these compounds in the X-band region to absorb radar waves.

Acknowledgments

The authors would like to represent their acknowledgments to the Science and Research branch of Islamic Azad University.

References

1. Veisi SS, Yousefi M, Amini M, Shakeri A, Bagherzadeh M, Afghahi SS. Magnetic properties, structural studies and microwave absorption performance of Ba0. 5Sr0. 5CuxZrxFe12-2xO19/Poly Ortho-Toluidine (X= 0.2, 0.4, 0.6, 0.8) ceramic nanocomposites. Inorganic Chemistry Communications. 2021;132:108802.

2. Yousefi M, Afghahi S, Amini M, Torbati MB. An investigation of structural and magnetic properties of Ce–Nd doped strontium hexaferrite nanoparticles as a microwave absorbent. Materials Chemistry and Physics. 2019;235:121722.

3. Alimoradi M, Yousefi M, Sadeghi B, Amini M, Abbasi A. Structural and Magnetic Behavior of BaAlxCryFe11O19 (x+ y= 1) Hexagonal Ferrites. Journal of Superconductivity and Novel Magnetism.2019;32(8):2533-8.

4. Haq A, Anis-ur-Rehman M. Effect of Pb on structural and magnetic properties of Ba-hexaferrite. Physica B: Condensed Matter. 2012;407(5):822-6.

5. Ansari M, Bigham A, Hassanzadeh-Tabrizi S, Ahangar HA. Synthesis and characterization of Cu0. 3Zn0. 5Mg0. 2Fe2O4 nanoparticles as a magnetic drug delivery system. Journal of Magnetism and Magnetic Materials. 2017;439:67-75.

6. Sadiq I, Naseem S, Ashiq MN, Khan M, Niaz S, Rana M. Structural and dielectric properties of doped ferrite nanomaterials suitable for microwave and biomedical applications. Progress in Natural Science: Materials International. 2015;25(5):419-24.

7. Beheshti KA, Yousefi M. Impact of Mg-Zr substitution on the magnetic and microwave absorption properties of BaFe12-2xMgxZrxO19 (0.25≤ x≤ 1.5). International Journal of Applied Ceramic Technology. 2020;17(5):2240-9.

8. Hong X, Xie Y, Wang X, Li M, Le Z, Gao Y, et al. A novel ternary hybrid electromagnetic waveabsorbing composite based on BaFe11. 92 (LaNd) 0.04 O19-titanium dioxide/multiwalled carbonnanotubes/polythiophene. Composites Science and Technology. 2015;117:215-24.

9. Abbas W, Ahmad I, Kanwal M, Murtaza G, Ali I, Khan MA, et al. Structural and magnetic behavior of Pr-substituted M-type hexagonal ferrites synthesized by sol–gel autocombustion for a variety of applications. Journal of Magnetism and Magnetic Materials. 2015;374:187-91.

10. Trukhanov A, Astapovich K, Almessiere M, Turchenko V, Trukhanova E, Korovushkin V, et al. Pecularities of the magnetic structure and microwave properties in Ba (Fe1-xScx) 12O19 (x< 0.1) hexaferrites. Journal of Alloys and Compounds. 2020;822:153575.

11. Beheshti KA, Yousefi M. Magnetic and microwave absorption of BaMgxZrxFe12-2xO19 polyaniline nanocomposites. Journal of Alloys and Compounds. 2021;859:157861.

12. Ghezelbash S, Yousefi M, Hossainisadr M, Baghshahi S. Structural and magnetic properties of Sn 4+ doped strontium hexaferrites prepared via sol–gel auto-combustion method. IEEE Transactions on Magnetics. 2018;54(9):1-6.

13. Nandotaria RA, Jotania RB, Sandhu CS, Hashim M, Meena SS, Bhatt P, Shirsath SE. Magnetic interactions and dielectric dispersion in Mg substituted M-type Sr-Cu hexaferrite nanoparticles prepared using one step solvent free synthesis technique. Ceramics International. 2018;44(4):4426-35.

14. Afghahi SSS, Peymanfar R, Javanshir S, Atassi Y, Jafarian M. Synthesis, characterization and microwave characteristics of ternary nanocomposite of MWCNTs/doped Sr-hexaferrite/PANI. Journal of Magnetism and Magnetic Materials. 2017;423:152-7.

15. Singh J, Singh C, Kaur D, Zaki H, Abdel-Latif I, Narang SB, et al. Elucidation of phase evolution, microstructural, Mössbauer and magnetic properties of Co2+ Al3+ doped M-type BaSr hexaferrites synthesized by a ceramic method. Journal of Alloys and Compounds. 2017;695:1112-21.

16. Narang SB, Kaur P, Bahel S. Complex permittivity, permeability and microwave absorbing properties of Co–Ti substituted strontium hexaferrite. Materials Science-Poland. 2016;34(1):19-24.

17. Mesdaghi S, Yousefi M, Mahdavian A. The effect of PANI and MWCNT on magnetic and photocatalytic properties of substituted barium hexaferrite nanocomposites. Materials Chemistry and Physics. 2019;236:121786.

18. Shlyk L, Vinnik D, Zherebtsov D, Hu Z, Kuo C-Y, Chang C-F, et al. Single crystal growth, structural characteristics and magnetic properties of chromium substituted M-type ferrites. Solid State Sciences. 2015;50:23-31.

19. Iqbal MJ, Ashiq MN, Gul IH. Physical, electrical and dielectric properties of Ca-substituted strontium hexaferrite (SrFe12O19) nanoparticles synthesized by co-precipitation method. Journal of Magnetism and Magnetic Materials. 2010;322(13):1720-6.

20. Datta A, Chakraborty S, Mukherjee S, Mukherjee S. Synthesis of carbon nanotube (CNT)-BiFeO3 and (CNT)-Bi2Fe4O9 nanocomposites and its enhanced photocatalytic properties. International Journal of Applied Ceramic Technology. 2017;14(4):521-31.

21. Liu X, Zhong W, Yang S, Yu Z, Gu B, Du Y. Structure and magnetic properties of La3+-substituted strontium hexaferrite particles prepared by sol–gel method. physica status solidi (a). 2002;193(2):314-9.

22. Yousefi M, Alimard P. Synthesis of M–Nd doped Fe3O4 nanoparticles (M= Co, Ce, Cr, Ni) with tunable magnetic properties. Bulletin of the Chemical Society of Ethiopia. 2013;27(1):49-56.

23. Das J, Moholkar VS, Chakma S. Structural, magnetic and optical properties of sonochemically synthesized Zr-ferrite nanoparticles. Powder Technology. 2018;328:1-6.

24. Baykal A, Güngüneş H, Sözeri H, Amir M, Auwal I, Asiri S, et al. Magnetic properties and Mössbauer spectroscopy of Cu-Mn substituted BaFe12O19 hexaferrites. Ceramics International. 2017;43(17):15486-92.

25. Alange R, Khirade PP, Birajdar SD, Humbe AV, Jadhav K. Structural, magnetic and dielectrical properties of Al–Cr Co-substituted M-type barium hexaferrite nanoparticles. Journal of Molecular Structure. 2016;1106:460-7.

26. Jayakumar T, Ramachandra Raja C, Arumugam S. Elucidation of structural, optical, and magnetic properties of Cd/Ni-doped strontium hexaferrite. Journal of Materials Science: Materials in Electronics.2020;31(19):16308-13.

27. Pahwa C, Mahadevan S, Narang SB, Sharma P. Structural, magnetic and microwave properties of exchange coupled and non-exchange coupled BaFe12O19/NiFe2O4 nanocomposites. Journal of Alloys and Compounds. 2017;725:1175-81.